Chinese Medical Journal Pulmonary and Critical Care Medicine 3 (2025) 308–318

Contents lists available at ScienceDirect

Chinese Medical Journal Pulmonary and Critical Care Medicine

journal homepage: www.elsevier.com/locate/pccm

Original Article

Enrichment of the commensal microbiome in the lower respiratory tract is associated with improved outcomes following lung transplantation

Chun Wang[a,1], Kang Chang[a,1], Mengyin Chen[b,1], Xiaohui Zou[a,1,*], Yawen Ni[c,d], Qing Zhang[a,c], Li Zhao[b], Bin Xing[b], Lijuan Guo[b], Wenhui Chen[b,**], Bin Cao[a,*]

[a] *National Center for Respiratory Medicine; State Key Laboratory of Respiratory Health and Multimorbidity; National Clinical Research Center for Respiratory Diseases; Institute of Respiratory Medicine, Chinese Academy of Medical Sciences; Laboratory of Clinical Microbiology and Infectious Diseases, Department of Pulmonary and Critical Care Medicine, Center of Respiratory Medicine, China–Japan Friendship Hospital, Beijing 100029, China*

[b] *National Center for Respiratory Medicine; State Key Laboratory of Respiratory Health and Multimorbidity; National Clinical Research Center for Respiratory Diseases; Institute of Respiratory Medicine, Chinese Academy of Medical Sciences; Department of Lung Transplantation, Center of Respiratory Medicine, China–Japan Friendship Hospital, Beijing 100029, China*

[c] *Chinese Academy of Medical Sciences and Peking Union Medical College, Beijing 100029, China*

[d] *Changping Laboratory, Beijing 100029, China*

ARTICLE INFO

Edited by: Peifang Wei

Keywords:
Lung transplantation
Metagenomics
Lower respiratory tract microbiome
Stability
Infection
Clinical outcomes

ABSTRACT

Background: Alterations in the respiratory microbiome are common following lung transplantation; however, the complex relationship between microbial composition and posttransplant clinical outcomes remains insufficiently characterized. This study aimed to delineate microbial signatures within the lower respiratory tract and to elucidate their associations with posttransplant outcomes in lung transplant recipients (LTRs).

Methods: Metagenomic sequencing was performed on 138 bronchoalveolar lavage fluid (BALF) samples collected in 2023 from patients who had undergone lung transplantation between 2017 and 2023 at the China–Japan Friendship Hospital. Lung function indices, hematologic parameters, and serum cytokine levels were assessed, and patients were prospectively followed to record adverse clinical events.

Results: The lung microbiome of stable LTRs formed four distinct clusters, exhibiting marked heterogeneity in both α- and β-diversity. The most prevalent cluster, enriched with oral-origin commensals, such as *Neisseria subflava* (*N. subflava*), *Prevotella melaninogenica*, and *Streptococcus mitis* (*S. mitis*), demonstrated the highest microbial diversity, and was associated with the lowest C-reactive protein levels, fewest adverse events, and the longest complication-free postoperative duration. In contrast, a virus-enriched cluster characterized by reduced diversity and high abundance of *Torque teno virus* and *Cytomegalovirus human betaherpesvirus 5* was associated with poorer outcomes. BALF samples from infected LTRs exhibited more severe dysbiosis than those from immunocompetent individuals, with reduced diversity and pathogen dominance. Concurrent infections aggravated antibody-mediated rejection-related lung function decline, indicating complex microbiome–immune interactions. Integrative modeling of microbiome, hematologic, and pulmonary function data yielded superior diagnostic performance for infection detection (area under the receiver operating characteristic curve = 0.93).

Conclusion: The composition of the lung microbiome may serve as a prognostic biomarker for clinical outcomes after lung transplantation. The presence of diverse, commensal-dominated communities was associated with improved outcomes, whereas viral enrichment correlated with adverse events. These findings underscore the clinical importance of microbiome monitoring in posttransplant management and suggest that targeted modulation of microbial communities could improve long-term graft stability and patient prognosis.

* Corresponding author at: Department of Pulmonary and Critical Care Medicine, Center of Respiratory Medicine, China–Japan Friendship Hospital, No. 2, Yinghua East Street, Chaoyang District, Beijing 100029, China.

** Corresponding authors at: Department of Lung Transplantation, Center of Respiratory Medicine, China–Japan Friendship Hospital, No. 2, Yinghua East Street, Chaoyang District, Beijing 100029, China.

E-mail addresses: zouxiaohui17@163.com (X. Zou), wenhuichen1004@sina.com (W. Chen), caobin_ben@163.com (B. Cao)

[1] Chun Wang, Kang Chang, Mengyin Chen, and Xiaohui Zou contributed equally to this work.

https://doi.org/10.1016/j.pccm.2025.11.006
Received 6 May 2025; Available online 12 December 2025

Introduction

Lung transplantation represents the definitive therapeutic option for patients with end-stage respiratory diseases, most commonly interstitial lung disease, chronic obstructive pulmonary disease (COPD), and cystic fibrosis.[1] Despite continuous advances in surgical techniques and post-transplant management, the 5-year mortality rate among lung transplant recipients (LTRs) remains higher than that of recipients of other solid organ transplants.[2–5] This persistent survival gap highlights the need for a deeper understanding of the biological and clinical determinants influencing posttransplant outcomes.

The lung hosts a highly dynamic and diverse microbial ecosystem that plays a pivotal role in maintaining respiratory homeostasis and modulating immune responses, both in health and disease.[6–8] In comparison with healthy individuals, LTRs exhibit profound alterations in the lung microbiome, characterized by reduced α-diversity, depletion of beneficial commensals, such as Bacteroidetes and Firmicutes, and enrichment of potential pathogens, including Proteobacteria.[9–12] Emerging evidence suggests that these microbial disturbances may influence posttransplant immune regulation by altering the gene expression of local innate immune cells, thereby affecting airway remodeling, inflammation, and overall graft function.[13] Previous studies have associated lung microbiome perturbations and bacterial burden with allograft dysfunction and increased mortality risk.[9,11,14–21] However, the features of microbiome reestablishment during clinically stable posttransplant periods and their relationship with long-term clinical outcomes remain poorly defined. In addition to bacterial dysbiosis, the lung mycobiome and virome also undergo substantial changes in LTRs,[10,22,23] but their prognostic significance in the context of lung transplantation has yet to be elucidated.

Chronic immunosuppressive therapy further predisposes LTRs to opportunistic respiratory infections caused by bacteria,[24–26] viruses—particularly cytomegalovirus (CMV),[27] and fungi such as *Aspergillus* species.[28,29] These infections accelerate the decline in graft function and contribute substantially to morbidity and mortality following transplantation.[17,24,30–32] Although the critical role of the lung microbiome in transplant outcomes is increasingly recognized, limited research has focused on microbial alterations accompanying posttransplant infections. The dynamic shifts in microbial community structure and their interplay with infection-associated allograft injury remain largely unexplored.

To address these knowledge gaps, this study comprehensively characterized the lower respiratory tract microbiome in stable and infected LTRs using metagenomic next-generation sequencing (mNGS) of bronchoalveolar lavage fluid (BALF). We hypothesized that (1) the lung microbiome of clinically stable LTRs reestablishes a balanced state whose degree of restoration correlates with clinical prognosis and (2) LTRs with active infections exhibit a more pronounced dysbiosis that contributes to infection identification and may elucidate mechanisms of allograft dysfunction. To test these hypotheses, we analyzed 138 BALF samples collected in 2023 from patients who had undergone lung transplantation between 2017 and 2023 at the China–Japan Friendship Hospital, defining the microbial characteristics of LTRs and their associations with clinical outcomes.

Methods

Ethical approval

The study received approval from the Clinical Research Ethics Committee of the China–Japan Friendship Hospital (approval number 2023-KY-043). All procedures involving human participants were conducted in accordance with institutional and national ethical standards and the principles of the *Declaration of Helsinki*. Informed consent was obtained from all participants before inclusion in the study. Voluntary consent, free from coercion, was obtained from all donors or their next of kin. No donor lungs were procured from executed prisoners or prisoners of conscience.

Study design and sample collection

This exploratory study enrolled patients who underwent lung transplantation and were treated at the China–Japan Friendship Hospital between March and December 2023. Clinical diagnoses were established according to the 2016 International Society for Heart and Lung Transplantation (ISHLT) Diagnostic Guidelines for Antibody-Mediated Rejection (AMR) and the 2010 International Society for Heart and Lung Transplantation (ISHLT) Diagnostic Guidelines for Infection.[33,34] Clinical stability was defined by the absence of clinical or radiographic evidence of infection and rejection. Based on diagnostic and clinical status, samples were categorized into four groups: (1) clinically stable (non-event) patients, (2) infection cases, (3) AMR, and (4) AMR with concurrent infection.

A total of 159 postoperative BALF samples were collected from 128 patients, together with 14 preserved saline samples used as negative controls. All samples were subjected to metagenomic sequencing (Supplementary Fig. 1). Exclusion criteria were: (1) patient age < 18 years, (2) BALF collected within 3 weeks postsurgery, and (3) samples yielding fewer than 600 microbial sequencing reads. In parallel, 148 blood samples were obtained for complete blood count, C-reactive protein (CRP), and procalcitonin (PCT) measurement. Blood samples were collected as close as possible to BALF sampling according to clinical indications, with 89.9 % (133/148) collected within 3 days and the remainder within 1 week. Eleven paired samples were unavailable. Of the blood samples, 77 with sufficient volume were centrifuged to obtain plasma for cytokine assays.

Detailed demographic and clinical characteristics of the cohort are presented in Table 1. All recipients received standard triple immunosuppressive therapy consisting of tacrolimus, mycophenolate mofetil, and prednisone. Antimicrobial treatment administered within 1 month before sampling was recorded (Supplementary Table 1). All participants were prospectively followed up for 13.1 months (interquartile range [IQR]: 12.2–14.9 months) to document posttransplant complications and outcomes.

For comparison, an additional 28 BALF samples were collected from immunocompetent patients; their demographic and clinical data are summarized in Supplementary Table 2.

DNA extraction and metagenomic sequencing

DNA was extracted from BALF samples using the DNeasy PowerSoil Pro Kit (QIAGEN, Cat. No. 47016, Hilden, North Rhine-Westphalia, Germany). Metagenomic libraries were prepared with the QIAseq FX DNA Library Kit (QIAGEN, Cat. No. 180479). Shotgun sequencing was performed on the Illumina NovaSeq 6000 platform (Illumina, San Diego, CA, USA) using paired-end 150 bp reads, generating approximately 10 GB of raw data per sample.

Sequencing data analysis

Raw Illumina reads were processed using Fastp (v0.23.4, http://opengene.org/fastp/fastp.html) for quality control, including adapter trimming and removal of low-quality sequences with the parameters: (-l 50 -x -w 10 –detect_adapter_for_pe –overlap_len_require 20 –overlap_diff_limit 5 –overlap_diff_percent_limit 20 –cut_tail –cut_tail_mean_quality 15).[35] Contaminating human reads were eliminated using Kneaddata (v0.12.0, https://huttenhower.sph.harvard.edu/kneaddata/) with the parameters: (–bypass-trim –bypass-trf –reordear -v –remove-intermediate-output –max-memory 100 g –bowtie2-options –very-sensitive –dovetail), using the human reference genome (GRCh37).[36] Bacterial taxonomic profiling was performed using Kraken2 (v2.1.3, https://doi.org/10.5281/zenodo.3520272)

Table 1
Demographics and clinical characteristics of the study cohort.

Items	Total	Stable	Infection	AMR	AMR_Infection	Statistics	*P*-value
LTRs, *n*	121	42	66	7	6		
BALF, *n*	138	45	78	7	8		
Age (years), median (IQR)	61 (54–67)	61 (56–66)	61 (54–68)	58 (50–66)	59 (54–65)	0.71*	0.87
Male, *n* (%)	91 (75.2)	30 (71.4)	54 (81.8)	4 (57.1)	3 (50.0)	-	0.11†
Type of lung transplantation, *n* (%)							
Single	33 (27.3)	9 (21.4)	21 (31.8)	2 (28.6)	1 (16.7)	-	0.66†
Bilateral	88 (72.7)	33 (78.6)	45 (68.2)	5 (71.4)	5 (83.3)		
Postoperative duration (days), median (IQR)	525 (163–1147)	859 (405–1455)	318 (103–932)	750 (352–1135)	386 (260–629)	12.35*	0.01
Primary disease, *n* (%)						-	0.58†
ILD	90 (74.4)	28 (66.7)	52 (78.8)	6 (85.7)	4 (66.7)		
COPD	13 (10.7)	7 (16.7)	5 (7.6)	1 (14.3)	0 (0)		
Bronchiectasis	3 (2.5)	1 (2.4)	2 (3.0)	0 (0)	0 (0)		
Others‡	15 (12.4)	6 (14.3)	7 (10.6)	0 (0)	2 (33.3)		
Antimicrobial admission							
Anti_bacterial admission, *n/N* (%)	11/138 (8.0)	1/45 (2.2)	8/78 (10.3)	1/7 (14.3)	1/8 (12.5)	-	0.16†
Anti_fungal admission, *n/N* (%)	18/138 (13.0)	4/45 (8.9)	14/78 (17.9)	0/7 (0)	0/8 (0)	-	0.23†
Anti_viral admission, *n/N* (%)	12/138 (8.7)	1/45 (2.2)	9/78 (11.5)	1/7 (14.3)	1/8 (12.5)	-	0.14†
Immunosuppression, *n*	100.0	100.0	100.0	100.0	100.0	-	1.00†

AMR: Antibody-mediated rejection; BALF: Bronchoalveolar lavage fluid; COPD: Chronic obstructive pulmonary disease; ILD: Interstitial lung disease; IQR: Interquartile range; LTRs: Lung transplant recipients. *H value. † Fisher's exact test. ‡ Other primary diseases include bronchiolitis obliterans and chronic lung allograft dysfunction.

with parameters (–minimum-hit-groups 4 –confidence 0.1, v. 2.1.3), and Bracken (v2.9, http://ccb.jhu.edu/software/bracken/) against the National Center for Biotechnology Information (NCBI) nucleotide database (version 2024.02).[37,38] For viral identification, quality-filtered reads were merged and assembled with MEGAHIT (v1.2.9, https://github.com/voutcn/megahit) using the parameters (–min-contig-len 1000 –presets meta-large).[39] The assembled contigs were taxonomically annotated via BLASTN against the NCBI database (version 2024.02.08), retaining only viral hits. A custom viral database was subsequently constructed, and reads were aligned using Burrows-Wheeler Aligner (BWA) (v0.7.17-r1188, http://maq.sourceforge.net) with default settings.[40] Reads not assigned to bacterial or fungal taxa by Kraken2 were aligned to the viral database using BWA and further processed with Samtools (v1.18, http://samtools.sourceforge.net).[41] The bacterial, fungal, and viral taxonomic profiles were integrated for downstream compositional analysis. To minimize background interference, species whose relative abundances were less than five-fold higher than those in negative controls were designated as potential contaminants.[42]

Clustering analysis

Unsupervised clustering of stable LTRs' microbiota composition was conducted using *k*-means[43] and hierarchical clustering[44] algorithms based on the Jensen–Shannon distance (JSD) metric. Optimal cluster determination was guided by the silhouette method, which indicated four distinct clusters as the best fit, consistent with within-cluster variability analyses supporting both two- and four-cluster solutions.

Plasma cytokine measurements

Plasma cytokine concentrations were quantified using a 12-cytokine detection kit (RAISECARE, Qingdao, Shandong, China) on the RaiseCyte flow cytometry platform. This assay enabled simultaneous measurement of interleukins interleukin (IL)-1β, IL-2, IL-4, IL-5, IL-6, IL-8, IL-10, IL-12p70, IL-17, tumor necrosis factor-α (TNF-α), interferon-α (IFN-α), and interferon-γ (IFN-γ).

Hematologic parameter analysis

Hematologic indices were assessed using the Fluorocell WDF staining kit (Jilin Ruite Biotechnology Co., Ltd, Changchun, Jilin, China) and the SYSMEX XN-10x hematology platform (Sysmex Corporation, Shanghai, China). Measured parameters included white blood cell, neutrophil (NEU), and lymphocyte (LYM) counts, as well as prothrombin time and CRP concentrations.

Statistical analysis and visualization of data

Jensen–Shannon distance (JSD) metrics were computed using the philentropy R package (v0.5.0, https://cran.r-project.org/web/packages/philentropy/index.html),[45] yielding values from 0 (identical) to 1 (maximally distinct). Nonparametric tests, including the Kruskal-Wallis and Wilcoxon signed-rank tests, were applied for between-group comparisons of continuous variables with skewed distribution, with multiple testing corrections performed using the Benjamini–Hochberg false discovery rate procedure.[46] Fisher's exact test was employed to evaluate the differences in categorical variables. All statistical analyses were performed using R (https://www.R-project.org/). Results with P <0.05 were considered statistically significant. Antibiotic exposure within 1 month before sampling was included as a covariate to control for potential confounding effects. The relationship between clinical metrics and factors (age, sex, antimicrobial therapy, serum CRP concentrations, postoperative duration and so on) and overall microbial composition and diversity was evaluated using permutational multivariate analysis of variance (PERMANOVA) based on JSD. PERMANOVA was performed with 9999 permutations using the adonis2 function from the vegan R package (v2.5.7, https://github.com/vegandevs/vegan).[47] Differential abundance analysis was conducted using ZicoSeq (https://CRAN.R-project.org/package=GUniFrac), adjusting for age, sex, antimicrobial therapy, and postoperative duration.[48] The L1-regularized logistic regression model was employed to identify the microbiome, lung function, and blood cells that could discriminate between stable and infected long-term recipients (LTRs). Additionally, the area under the receiver operating characteristic curve (AUC) was utilized to evaluate the performance of the classifier. Microbial network architecture was compared between stable and infected LTRs using the NetCoMi R package (https://github.com/stefpeschel/NetCoMi),[49] assessing network topology and community-level interactions.

Results

Patient cohort and samples

A total of 121 LTRs were included in the study, comprising 91 men (75.2%) and 30 women (24.8%), with a median age of 61 years (IQR,

54–67 years). Among these patients, 33 underwent single-lung transplantation and 88 underwent bilateral procedures. The primary underlying diseases necessitating transplantation were interstitial lung disease (ILD, $n = 90$, 74.4 %), COPD ($n = 13$, 10.7 %), bronchiectasis ($n = 3$, 2.5 %), and other etiologies ($n = 15$, 12.4 %), as detailed in Table 1.

In total, 138 BALF samples were analyzed and stratified into four groups according to clinical classification: stable (non-event) cases, infection-only (infection), AMR, and AMR with concurrent infection (AMR_Infection). As summarized in Table 1, postoperative duration differed significantly among groups, demonstrating a clear trend toward earlier occurrence of infection following surgery.

Distinct clustering of the lower respiratory microbiota in stable lung transplant recipients

To characterize the lower respiratory tract microbiome among stable LTRs, unsupervised clustering analysis was performed using the *k*-means algorithm. Evaluation of within-cluster variability and silhouette width revealed that four clusters provided the optimal model fit for all 45 stable BALF samples at the species level (Supplementary Fig. 2A and B). These four clusters (Clusters 1–4) exhibited markedly different microbial compositions, as visualized by non-metric multidimensional scaling (NMDS; Fig. 1A, PERMANOVA $R^2 = 0.24$, $P = 0.001$ for β-diversity) and hierarchical clustering-based stacked bar plots (Supplementary Fig. 3). Alpha diversity analysis demonstrated that Clusters 1 and 2 exhibited significantly higher Shannon and Chao1 indices than Clusters 3 and 4 (Fig. 1B and C), indicating that the former two clusters harbored more diverse and compositionally balanced microbial communities. Core taxa, defined as species present in ≥50 % of samples with relative abundance >1 %, revealed distinct microbial signatures across clusters.

Cluster 1 ($n = 20$), the most prevalent and compositionally balanced group, was dominated by typical respiratory commensals, including *Neisseria subflava* (*N. subflava*), *Prevotella melaninogenica*, *Streptococcus mitis*, *Haemophilus parainfluenzae*, *Rothia mucilaginosa*, and *Streptococcus oralis* (Fig. 1D). Cluster 2 ($n = 13$) shared seven core taxa with Cluster 1 but displayed a pronounced enrichment of *Torque teno virus* (TTV), suggesting a distinctive viral influence within this subgroup. Cluster 3 ($n = 6$) was characterized by a virus-enriched microbial community, exhibiting high relative abundances of nonpathogenic TTV, Myoviridae species, and the pathogenic *Cytomegalovirus human betaherpesvirus 5*. Cluster 4 ($n = 6$) displayed the greatest microbial heterogeneity, featuring particularly high levels of *Corynebacterium striatum* (*C. striatum*) (mean relative abundance = 33.56 %). Collectively, these findings demonstrate substantial heterogeneity in the lower respiratory microbiome among clinically stable LTRs.

Commensal-dominated microbiota cluster in stable lung transplant recipients is associated with favorable clinical outcomes

We next examined the association between microbial features and clinical outcomes in LTRs. A significant association was identified between CRP levels ($n = 40$, PERMANOVA, $P < 0.001$) and microbial composition and diversity after adjustment for age, sex, and recent antimicrobial therapy. Notably, patients with Cluster 3—characterized by low α-diversity and viral enrichment—exhibited significantly higher CRP levels than those with Cluster 1 (Fig. 2A, Supplementary Fig. 4A). Postoperative duration also differed among the clusters, showing a progressive trend consistent with microbiome stabilization over time (Fig. 2B). Cluster 1 demonstrated the longest median postoperative duration of 1091 days (IQR: 841–1619 days), followed by Cluster 2 at 700 days (IQR: 361–777 days), and Cluster 3 at 392 days (IQR: 246–668 days). This gradient, coupled with distinct compositional profiles, suggested a temporal recovery of microbiome resilience following transplantation. Furthermore, higher microbial diversity, as indicated by the Shannon index, correlated with better preservation of lung diffusing capacity for carbon monoxide (single-breath lung diffusing capacity for carbon monoxide [$DLCO_{SB}$], $R^2 = 0.17$, $P = 0.021$, Supplementary Fig. 4B), supporting a potential link between microbiome diversity and pulmonary function.

To assess long-term outcomes, the incidence of adverse clinical events—including infections, rejection, and malignancy—was tracked for 12–16 months after sample collection ($n = 37$). Cluster 1, characterized by high α-diversity and a balanced, commensal-dominant composition, exhibited the most favorable outcomes, with the lowest event frequency (Fig. 2C). Remarkably, 62.5 % (10 of 16) of LTRs in Cluster 1 remained free of complications for more than 1 year. In contrast, patients belonging to Cluster 3, defined by viral enrichment and reduced α-diversity, experienced a greater mean number of adverse events (mean = 2) compared with other clusters, indicating a higher risk of unfavorable clinical trajectories. These findings establish clear associations between lung microbiome composition, systemic inflammation, and posttransplant outcomes in LTRs.

Altered lower respiratory tract microbiota and reduced diversity in infected lung transplant recipients

Infection represents the most frequent postoperative complication among LTRs. To elucidate the impact of infection on the lower respiratory tract microbiome, we compared the microbial profiles of LTRs with and without infection. Patients with infection exhibited markedly lower α-diversity at the species level than their stable counterparts ($P < 0.05$; Fig. 3A–B). This reduction in diversity was primarily driven by increased species dominance. Specifically, 38.5 % (30/78) of infected LTRs displayed microbial communities dominated by taxa with relative abundances exceeding 50 %, compared with only 6.7 % of stable LTRs (Fig. 3C). The dominant species contributing to this imbalance included *Pseudomonas aeruginosa* (*P. aeruginosa*) and *C. striatum* (Supplementary Fig. 5). Microbiota composition in infected BALF samples exhibited a more discrete and divergent distribution compared with stable samples (PERMANOVA $R^2 = 0.02$, $P = 0.003$; Fig. 3D). ZicoSeq differential abundance analysis revealed enrichment of potential pathogens—including *P. aeruginosa*, *C. striatum*, and the nonpathogenic TTV—in infected cases, whereas stable LTRs harbored higher relative abundances of commensal taxa such as *Prevotella melaninogenica*, *N. subflava*, *Haemophilus parainfluenzae*, *Streptococcus mitis*, *Veillonella atypica*, *Rothia mucilaginosa*, *Streptococcus oralis*, and *Schaalia odontolytica* ($P_{.adj}$ <0.1; median relative abundance > 0.01, Fig. 3E).

Microbial network analysis further demonstrated striking alterations in community structure between the stable and infected states (Fig. 4). Using network comparison based on the Jaccard index, significant differences were observed in both closeness centrality and eigenvector centrality of key taxa ($P < 0.05$), indicating substantial shifts in microbial connectivity patterns. The adjusted Rand index (ARI = 0.285, $P < 0.001$) confirmed distinct clustering structures between networks. Notably, in stable LTRs, a strong negative correlation was observed between protective commensals and pathogens such as *P. aeruginosa*, CMV, and TTV. This antagonistic relationship was largely disrupted during infection, suggesting that commensal microbes may inhibit pathogen colonization and proliferation under stable posttransplant conditions.

Marked differences in clinical parameters were also identified between stable and infected groups. LTRs with infection exhibited significantly lower lung function indices, including forced expiratory volume in 1 s (FEV_1), forced vital capacity (FVC), and diffusing capacity for carbon monoxide ($DLCO_{SB}$), compared with stable LTRs. These reductions were evident even when baseline lung function (i.e., the best posttransplant measurements) was considered, with the exception of baseline $DLCO_{SB}$ (Supplementary Fig. 6A–F). Hematologic analyses revealed that while total white blood cell and NEU counts were comparable between groups, infected patients demonstrated significantly reduced LYM counts (Supplementary Fig. 6G–I). Additionally, the proportion of NEUs and the NEU-to-LYM ratio were elevated in infected LTRs, consistent

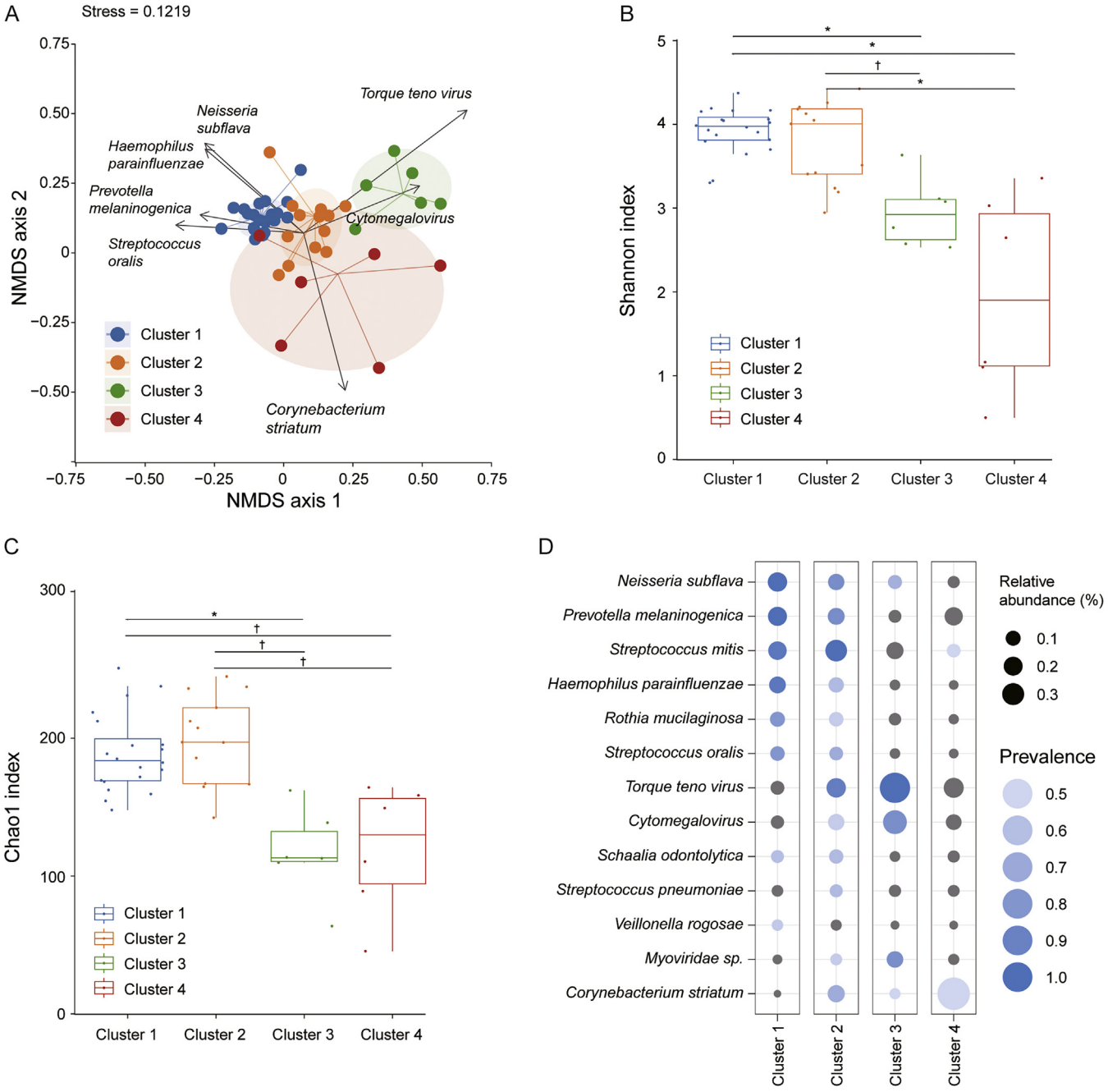

Fig. 1. Species-level microbial profiles of stable LTRs. (A) Nonmetric multidimensional scaling (NMDS) plot of lung microbiota in stable LTRs based on the Jensen–Shannon divergence distance at the species level. Samples are color-coded by clusters, with arrows indicating the seven species contributing most to variance in envfit analysis. Shaded regions represent the 95 % confidence intervals for each cluster. (B and C) Alpha diversity indices (Shannon and Chao1) in stable LTRs. * $P < 0.001$, † $P < 0.01$, Wilcoxon tests. (D) Bubble plots depicting the core microbiome composition and mean relative abundance across clusters. The *y*-axis lists microbial taxa at the species level, and the *x*-axis shows the four clusters (Clusters 1–4). Blue indicates taxa with >1 % abundance in ≥50 % of samples (core taxa), and gray indicates noncore taxa. Bubble sizes represent mean relative abundance within each cluster. LTRs: Lung transplant recipients.

with a predominant bacterial infection profile (Supplementary Fig. 6J and K).

To evaluate the infection diagnostic potential of these parameters, L_1-regularized logistic regression models were developed using microbiome, hematologic, and pulmonary function datasets, each subjected to five-fold cross-validation. To determine the advantage of multimodal integration, a combined model incorporating all three datasets was also constructed. Model performance was assessed by calculating the mean AUC across validation folds. Individually, each data domain achieved moderate diagnostic accuracy (AUC range 0.68–0.80), with microbiome data providing the highest standalone predictive performance (AUC = 0.80). Notably, the integrative model demonstrated superior accuracy, achieving an AUC of 0.93 (Fig. 3F; DeLong's test, $P < 0.01$).

Compromised respiratory microbiome stability in infected lung transplant recipients

To examine how lung transplantation influences respiratory microbiome dynamics during infection, we performed a comparative analysis of the lower respiratory tract microbiota between immunocompetent patients (IP) and LTRs experiencing infection. Infected LTRs exhibited

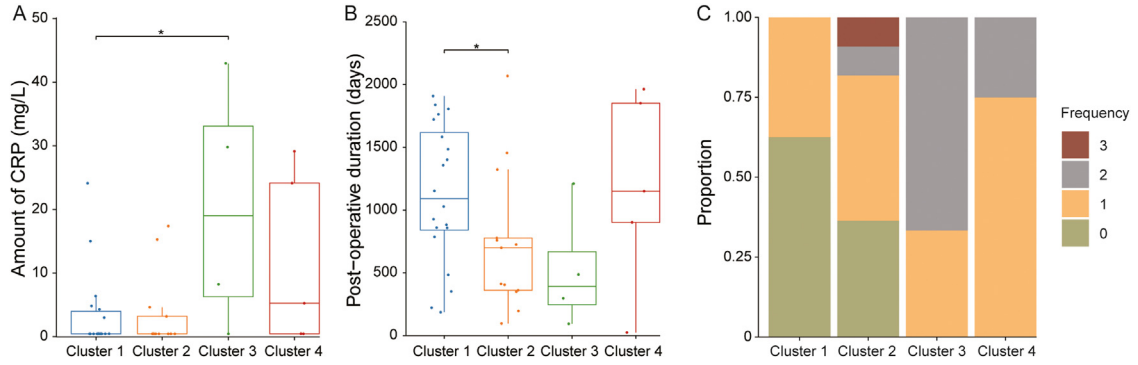

Fig. 2. Differences in clinical features across microbial clusters. (A) Serum C-reactive protein (CRP) levels and (B) postoperative duration across microbial clusters. * $P < 0.05$, Wilcoxon tests. (C) Frequency of adverse clinical episodes during 12–16 months among the four clusters.

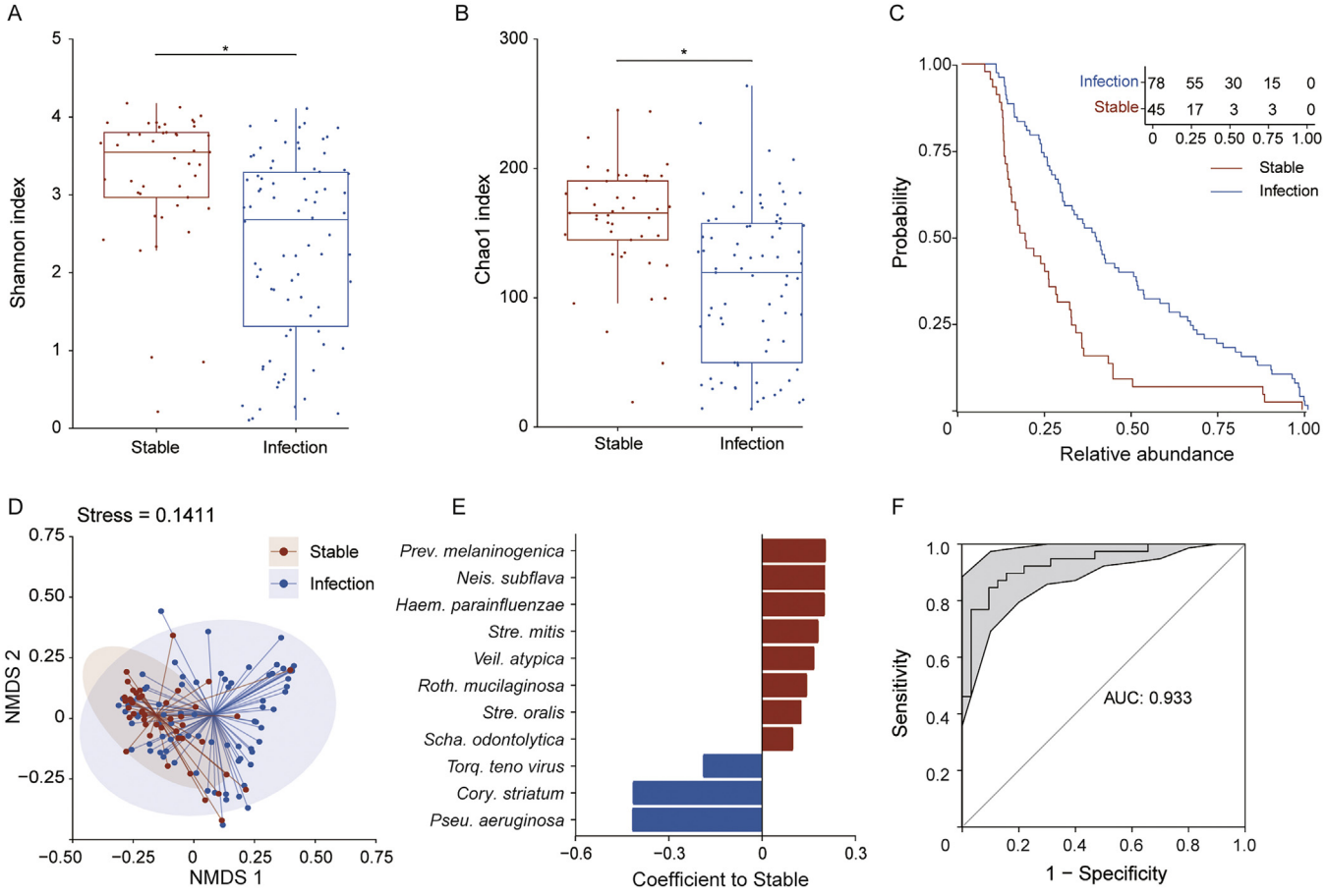

Fig. 3. Differences in BALF microbiota between stable and infected LTRs. (A and B) Alpha diversity indices (Shannon and Chao1) in stable and infected LTRs. * $P < 0.0001$, Wilcoxon tests. (C) Distribution of dominant microbes in stable and infected groups. The y-axis represents the proportion of patients in whom the relative abundance of the dominant microbe exceeds the threshold indicated on the x-axis. The difference between groups was statistically significant ($P < 0.001$, log-rank test). (D) NMDS plot of lung microbiota in stable and infected LTRs based on JSD distances. Shaded regions indicate 95 % confidence intervals. (E) Microbes with significantly different abundances between groups identified by ZicoSeq (P_{adj} <0.1; median relative abundance >1 %). (F) Receiver operating characteristic (ROC) curve of the L_1-regularized logistic regression classifier for infection diagnosis. The shaded area represents the 95% confidence interval of the AUC. The optimal cutoff was 0.538, with a sensitivity of 0.906 and a specificity of 0.846. AUC: Area under the receiver operating characteristic curve; BALF: Bronchoalveolar lavage fluid; *Cory. striatum: Corynebacterium striatum; Haem. parainfluenzae: Haemophilus parainfluenzae*; JSD: Jensen–Shannon distance; LTRs: Lung transplant recipients; *Neis. subflava: Neisseria subflava*; NMDS: Nonmetric multidimensional scaling; *Prev. melaninogenica: Prevotella melaninogenica; Pseu. aeruginosa: Pseudomonas aeruginosa; Roth. mucilaginosa: Rothia mucilaginosa; Scha. odontolytica: Schaalia odontolytica; Stre. mitis: Streptococcus mitis; Stre.oralis: Streptococcus oralis; Torq. teno virus:* Torque teno virus; *Veil. atypica: Veillonella atypica*.

significant alterations in microbial community structure relative to infected immunocompetent individuals. Specifically, LTRs with infection showed a trend toward reduced α-diversity (Fig. 5A) and pronounced shifts in β-diversity ($P = 0.001$; Fig. 5B), reflecting a distinct microbial community composition. Furthermore, the JSD between infected and stable samples within the LTR cohort was significantly greater than the corresponding JSD values between infected and noninfected samples within the immunocompetent cohort (Fig. 5C). These findings suggest that lung transplantation compromises the stability and resilience of the lower respiratory tract microbiome during infection.

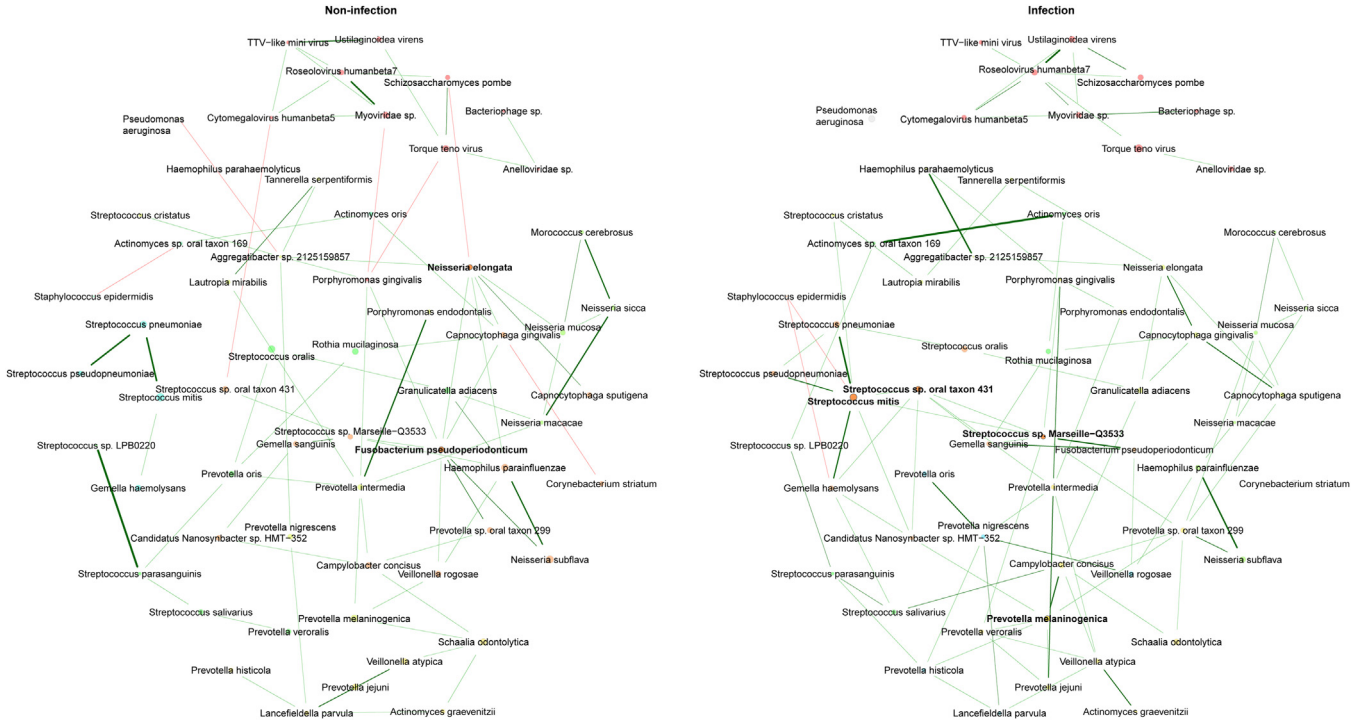

Fig. 4. Microbial interaction networks in stable and infected LTRs. The left and right panels depict microbial networks in stable and infected groups, respectively. Node size corresponds to modified centered log-ratio (MCLR)-transformed abundance. Green edges represent positive associations, and red edges indicate negative associations. Identical layouts were applied for both networks, with unconnected nodes removed for clarity. LTRs: Lung transplant recipients; TTV: *Torque teno virus*.

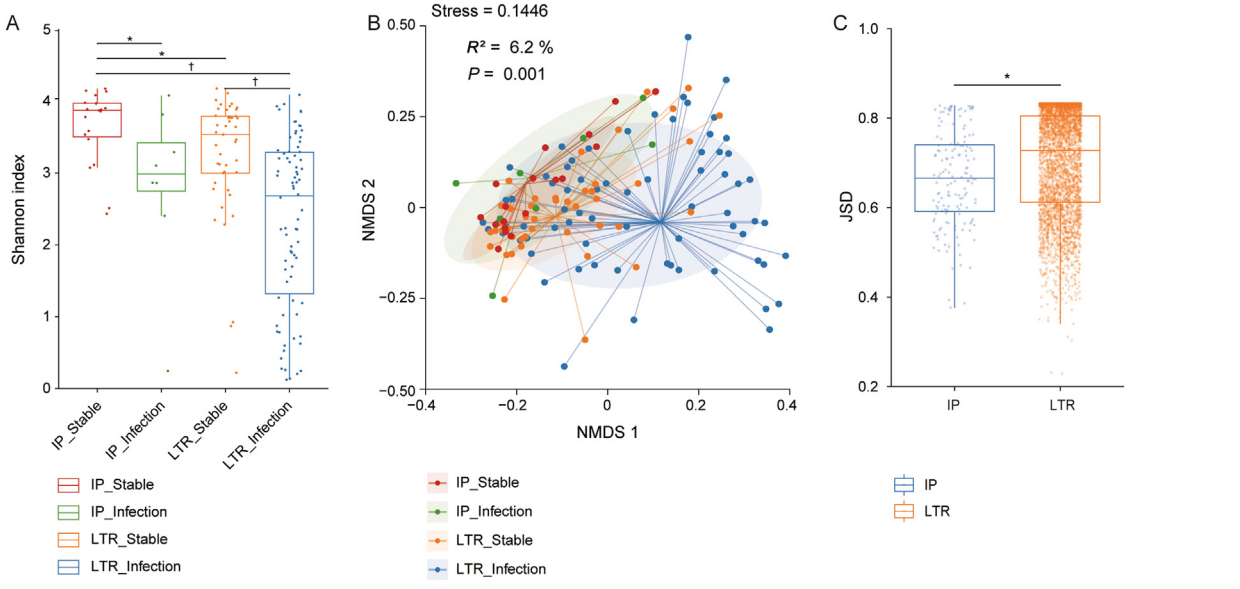

Fig. 5. Lung microbiota characteristics in lung transplant recipients (LTRs) and immunocompetent patients. (A) Alpha diversity (Shannon index). (B) Non-metric multidimensional scaling (NMDS) plot illustrating β-diversity (Jensen–Shannon distances [JSDs]) among bronchoalveolar lavage fluid (BALF) samples from two patient populations: immunocompetent patients (IP) in both stable and infected states, and LTRs in stable and infected conditions. Diversity metrics were calculated at the species level. (C) JSD at the species level between stable and infected patients within LTRs and IPs, respectively. Statistical significance was assessed using the Wilcoxon rank-sum test (* $P < 0.05$, † $P < 0.0001$).

Concurrent infection exacerbates the impact of AMR on lung function in lung transplant recipients

After characterizing the infection-associated microbiome alterations in LTRs, we further explored a distinct clinical context—concurrent infections in the setting of AMR. Among the various types of allograft rejection identified in our cohort, AMR was the most prevalent (15/128, 11.7 %), followed by chronic lung allograft dysfunction (CLAD; 12/128, 9.4 %) and acute cellular rejection (ACR; 5/128, 3.9 %). Of the 17 BALF samples collected from patients with AMR, 10 (58.8 %) were obtained during active infection, underscoring the high susceptibility of patients with AMR to concurrent infectious complications. We next compared microbiome and clinical features between patients with AMR with infection and those with infection alone. Lung function decline was assessed

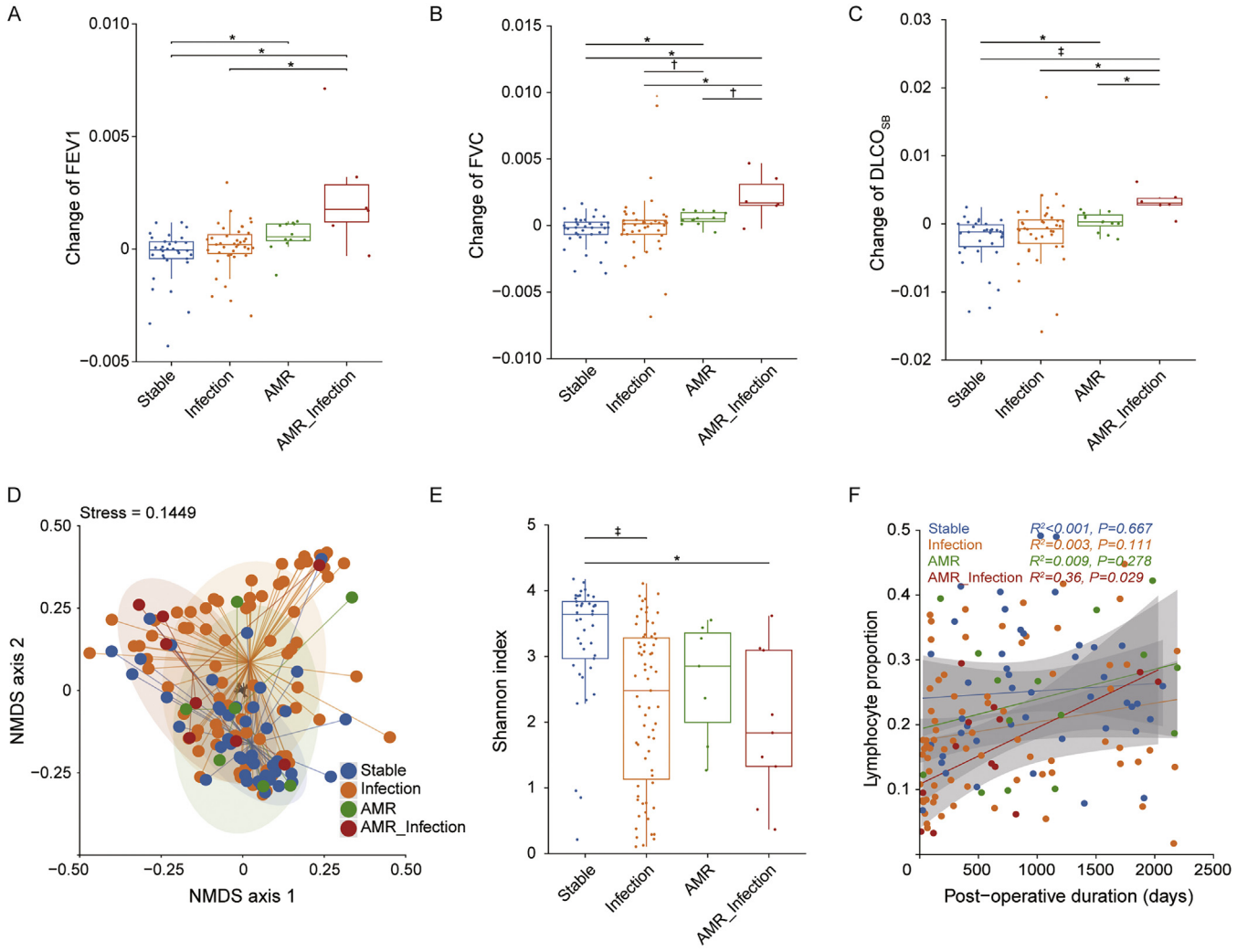

Fig. 6. Clinical characteristics and microbiome composition in LTRs with AMR and concurrent infection. (A–C) Boxplots showing adjusted changes in FEV_1 (A), FVC (B), and $DLCO_{SB}$ (C) across groups. Changes were calculated by subtracting the measurement at sampling from the mean of the two best posttransplant values. To minimize the influence of varying postoperative intervals, changes in pulmonary function parameters (FEV_1, FVC, and $DLCO_{SB}$) were normalized by postoperative duration, yielding adjusted values. Statistical comparisons were performed using the Wilcoxon test (* $P<0.01$, † $P<0.05$, ‡ $P<0.0001$). (D) NMDS plot of lung microbiota in LTRs among stable, infection, AMR, and AMR_Infection groups based on JSD distances at the species level. Shaded regions represent the 95 % confidence intervals for each cluster. (E) Shannon index values in stable, infection, AMR, and AMR_Infection groups. * $P<0.01$, ‡ $P<0.0001$. (F) Temporal dynamics of lymphocyte proportions across postoperative duration in stable, infection, AMR, and AMR_Infection groups. AMR: Antibody-mediated rejection; $DLCO_{SB}$: Single-breath lung diffusing capacity for carbon monoxide; FEV_1: Forced expiratory volume in 1 s; FVC: Forced vital capacity; JSD: Jensen–Shannon distance; LTRs: Lung transplant recipients; NMDS: Nonmetric multidimensional scaling.

as the difference between baseline pulmonary function—defined as the mean of the two best post-transplant measurements—and actual lung function at the time of sampling, adjusted for postoperative duration. Patients with infection alone did not exhibit significant reductions in lung function compared with stable cases; those with concurrent AMR and infection experienced a greater decline in FVC and $DLCO_{SB}$ than AMR-only and infection-only groups, and a greater decline in FEV_1 than infection-only group (Fig. 6A–C). These findings suggest that infection amplifies allograft injury in the context of AMR. Subsequent microbial profiling revealed that the AMR-with-infection group and the infection-only group shared similar microbial characteristics in the lower respiratory tract. Compared with stable BALF samples, both groups displayed significantly reduced α-diversity and marked compositional shifts, yet no statistically significant differences were observed between them (Fig. 6D and E). This indicates that microbiome alterations alone are insufficient to explain the extent of lung function deterioration in patients with concurrent AMR and infection. To further elucidate immune dynamics, we analyzed peripheral immune cell parameters. Absolute NEU and LYM counts did not differ significantly among groups. However, after accounting for postoperative duration, a temporal trend emerged: the proportion of LYMs in the AMR-with-infection group increased significantly over time, whereas NEU proportions gradually declined (Fig. 6F, Supplementary Fig. 7). These findings suggest that concurrent AMR and infection may be associated with dysregulated immune activation.

Discussion

This study provides a comprehensive characterization of the lower respiratory tract microbiome in LTRs and elucidates its association with post-transplant clinical outcomes and systemic inflammatory profiles. Through culture-independent mNGS and unsupervised clustering of BALF samples, we delineated four distinct microbial community clusters in clinically stable LTRs. These clusters captured both taxonomic diversity and compositional heterogeneity, revealing significant correlations between microbial architecture, immune activation, and patient prognosis.

A clear gradient emerged across Clusters 3, 2, and 1, characterized by progressive enrichment of commensal respiratory taxa—including *N. subflava*, *Prevotella melaninogenica*, and *Streptococcus* spp.—alongside a concomitant reduction in viral abundance (notably TTV) and increasing α-diversity. This continuum suggests a potential ecological succession of the lower respiratory microbiome, with gradual restoration of community balance following transplantation. The observed clustering patterns likely reflect complex posttransplant ecological dynamics, influenced by multiple factors such as diminishing donor-derived microbial influence, decreased prophylactic antibiotic exposure, withdrawal of intensive respiratory support, resumption of physical activity, environmental recolonization, microbial migration from the upper airway, and evolving host immune status.[50] Collectively, these findings provide novel insights into the adaptive reconstitution of respiratory microbial communities in the immunosuppressed posttransplant setting.

The enrichment of oral-origin commensals—including *N. subflava*, *Prevotella melaninogenica*, and *Streptococcus* spp.—in patients with favorable outcomes supports a potential protective role for these taxa. Such commensals may contribute to the maintenance of epithelial barrier integrity, modulation of local immune homeostasis, and competitive inhibition of pathogenic colonization, consistent with previous studies.[51,52] In contrast, the dominance of viral species such as TTV in low-diversity clusters, together with elevated systemic inflammatory markers and increased incidence of adverse clinical events, suggests a state of immune dysregulation. TTV has been recognized as a biomarker of immunosuppression and allograft tolerance, with elevated serum TTV levels reflecting heightened immunosuppressant exposure in LTRs.[53–56] However, its role within the lung microenvironment remains poorly defined. In this study, increased TTV abundance in BALF correlated with a higher incidence of post-transplant infection, suggesting that excessive local viral replication may mirror or contribute to an oversuppressed immune milieu, thereby facilitating secondary microbial invasion. Furthermore, the observed inverse correlation between TTV levels and commensal bacterial abundance implies that viral proliferation may perturb microbial community equilibrium, particularly under conditions of impaired immune surveillance.

Moreover, integrating microbiome, hematologic, and pulmonary function data yields superior diagnostic performance in LTRs, where infection diagnosis is often complex and reliant on traditional tests and clinical experience, highlighting the advantages of this multimodal approach. This index is increasingly feasible in practice: hematologic parameters and pulmonary function tests are routinely available, and the growing use of metagenomic pathogen detection can simultaneously provide microbiome information. The protective role of diverse, commensal-dominated microbial communities further suggests that microbiome-targeted interventions—such as prebiotic, probiotic, or microbiota-preserving therapeutic strategies—could help prevent adverse outcomes and promote long-term graft stability.

Our study provides compelling evidence of the profound impact of infection on the posttransplant respiratory microbiome. Infected LTRs exhibited significantly reduced α-diversity and pronounced shifts in microbial community structure, characterized by the overrepresentation of opportunistic pathogens such as *P. aeruginosa* and *C. striatum*.[57] These findings underscore the heightened susceptibility of immunosuppressed hosts to opportunistic infections and the potential of such infections to disrupt the delicate microbial equilibrium within the transplanted lung. The loss of negative correlations between commensals and pathogens observed in infected versus stable LTRs suggests that beneficial taxa may normally contribute to respiratory health through mechanisms such as competitive exclusion, nutrient limitation, and immune modulation.[58] From a clinical perspective, these observations support the inclusion of microbiome profiling in posttransplant surveillance algorithms. Quantitative changes of commensal abundance, alongside the detection of emerging pathogens or viral proliferation, may serve as early biomarkers of allograft instability or impending infection. Furthermore, our integrated diagnostic model—combining microbial, inflammatory, and physiological indices—achieved high accuracy in distinguishing infection states and offers a potential framework for individualized risk stratification and precision monitoring in transplant medicine.

Comparative analyses between infected LTRs and infected immunocompetent individuals revealed a destabilizing effect of lung transplantation on the respiratory microbiome. The significantly greater interindividual variability (as indicated by higher JSD) among infected LTRs reflects a reduced capacity to maintain microbial homeostasis, likely attributable to chronic immunosuppression, impaired mucosal defense, and the immunologic complexity of allograft acceptance. This reduced microbiome stability may contribute to the increased infection susceptibility and recurrent microbial perturbations characteristic of the posttransplant population.

This study also identified a complex interplay between infection, AMR, and pulmonary function. Patients with concurrent AMR and infection exhibited a more pronounced deterioration in lung function compared with those experiencing infection alone. Despite similar microbiome compositions between these groups, the combined presence of AMR and infection led to greater physiological impairment, suggesting that immune dysregulation—rather than microbiota composition per se—drives this exacerbation.[59] The longitudinal increase in LYM proportion and concomitant decline in NEUs in the AMR-with-infection group further imply an aberrant immune activation pattern, meriting deeper mechanistic exploration.

Several limitations warrant consideration. First, the substantial presence of host DNA in BALF samples limited the functional metagenomic analyses, underscoring the need for optimized host DNA depletion strategies to enhance microbial signal recovery. Second, the cross-sectional metagenomic detection precluded temporal assessment of microbiome dynamics and causal inference. Finally, the modest sample size, particularly within the AMR subgroup, constrains statistical power. Future research should employ longitudinal, multicenter cohorts and complementary experimental models to validate and extend these findings.

In conclusion, this study elucidates the pivotal role of the lung microbiome in shaping posttransplant outcomes and highlights the clinical relevance of microbial diversity and composition in graft health. Restoration and maintenance of a stable, commensal-enriched microbiome may represent a promising therapeutic avenue for improving long-term prognosis in LTRs. Future investigations should focus on developing targeted interventions that foster beneficial microbial communities and delineate the mechanistic pathways linking microbiome dysbiosis to immune dysregulation and graft dysfunction.

Author statement

The author Bin Cao is the Associate Editor for this journal and was not involved in the editorial review or the decision to publish this article.

Data availability

Sequencing data generated in this study have been deposited in the Genome Sequence Archive of the National Genomics Data Center, China National Center for Bioinformation, under accession number PRJCA031809 and are publicly accessible at https://bigd.big.ac.cn/gsa. The preview link is https://ngdc.cncb.ac.cn/gsa/s/1m86TOO3.

Funding

This research was supported by the National Key Research & Development Program of China (No. 2022YFA1304303), National High Level Hospital Clinical Research Fund (Nos. 2025-NHLHCRF-JBGS-B-WZ-06, 2022-NHLHCRF-LX-03-05, and 2022-NHLHCRF-LX-01), and the Chinese Academy of Medical Sciences (CAMS) Innovation Fund for Medical Sciences (No. 2021-I2M-1-049), and New Cornerstone Science Foundation.

Declaration of competing interest

The authors declare that they have no known competing financial interests or personal relationships that could have appeared to influence the work reported in this paper.

CRediT authorship contribution statement

Chun Wang: Writing – original draft, Formal analysis, Data curation. **Kang Chang:** Project administration, Data curation, Conceptualization. **Mengyin Chen:** Resources, Project administration, Investigation, Data curation, Conceptualization. **Xiaohui Zou:** Writing – review & editing, Conceptualization. **Yawen Ni:** Methodology. **Qing Zhang:** Project administration, Methodology. **Li Zhao:** Resources, Project administration. **Bin Xing:** Resources, Project administration. **Lijuan Guo:** Resources, Project administration. **Wenhui Chen:** Writing – review & editing, Funding acquisition, Conceptualization. **Bin Cao:** Writing – review & editing, Funding acquisition, Conceptualization.

Supplementary materials

Supplementary material associated with this article can be found, in the online version, at doi:10.1016/j.pccm.2025.11.006.

References

1. Kumar A, Sharma S, Anjum F. *StatPearls*. Lung transplantation. 2024 Jun 8. In: StatPearls [Internet]. Treasure Island (FL): StatPearls Publishing; 2025.
2. Valapour M, Lehr CJ, Schladt DP, et al. OPTN/SRTR 2022 annual data report: Lung. *Am J Transplant*. 2024;24:S394–S456. doi:10.1016/j.ajt.2024.01.017.
3. McCort M, MacKenzie E, Pursell K, Pitrak D. Bacterial infections in lung transplantation. *J Thorac Dis*. 2021;13:6654–6672. doi:10.21037/jtd-2021-12.
4. Martin-Gandul C, Mueller NJ, Pascual M, Manuel O. The impact of infection on chronic allograft dysfunction and allograft survival after solid organ transplantation. *Am J Transplant*. 2015;15:3024–3040. doi:10.1111/ajt.13486.
5. Gongtao Q, Xiaoshan L, Chunxiao H, Jingyu C. Interpretation of report on lung transplantation development in China 2021. *Chin J Front Med Sci*. 2023;15:76–87. doi:10.12037/YXQY.2023.04-01.
6. Natalini JG, Singh S, Segal LN. The dynamic lung microbiome in health and disease. *Nat Rev Microbiol*. 2023;21:222–235. doi:10.1038/s41579-022-00821-x.
7. Pirozzolo I, Li Z, Sepulveda M, Alegre ML. Influence of the microbiome on solid organ transplant survival. *J Heart Lung Transplant*. 2021;40:745–753. doi:10.1016/j.healun.2021.04.004.
8. Guo Y, Wang Q, Li D, et al. Vendor-specific microbiome controls both acute and chronic murine lung allograft rejection by altering CD4(+) Foxp3(+) regulatory T cell levels. *Am J Transplant*. 2019;19:2705–2718. doi:10.1111/ajt.15523.
9. Charlson ES, Diamond JM, Bittinger K, et al. Lung-enriched organisms and aberrant bacterial and fungal respiratory microbiota after lung transplant. *Am J Respir Crit Care Med*. 2012;186:536–545. doi:10.1164/rccm.201204-0693OC.
10. Young JC, Chehoud C, Bittinger K, et al. Viral metagenomics reveal blooms of anelloviruses in the respiratory tract of lung transplant recipients. *Am J Transplant*. 2015;15:200–209. doi:10.1111/ajt.13031.
11. Eskind CC, Shilts MH, Shaver CM, Das SR, Satyanarayana G. The respiratory microbiome after lung transplantation: Reflection or driver of respiratory disease. *Am J Transplant*. 2021;21:2333–2340. doi:10.1111/ajt.16568.
12. Borewicz K, Pragman AA, Kim HB, Hertz M, Wendt C, Isaacson RE. Longitudinal analysis of the lung microbiome in lung transplantation. *FEMS Microbiol Lett*. 2013;339:57–65. doi:10.1111/1574-6968.12053.
13. Bernasconi E, Pattaroni C, Koutsokera A, et al. Airway microbiota determines innate cell inflammatory or tissue remodeling profiles in lung transplantation. *Am J Respir Crit Care Med*. 2016;194:1252–1263. doi:10.1164/rccm.201512-2424OC.
14. Schneeberger P, Zhang C, Santilli J, et al. Lung allograft microbiome association with gastroesophageal reflux, inflammation, and allograft dysfunction. *Am J Respir Crit Care Med*. 2022;206:1495–1507. doi:10.1164/rccm.202110-2413OC.
15. Combs MP, Wheeler DS, Luth JE, et al. Lung microbiota predict chronic rejection in healthy lung transplant recipients: a prospective cohort study. *Lancet Respir Med*. 2021;9:601–612. doi:10.1016/S2213-2600(20)30405-7.
16. Natalini JG, Wong KK, Nelson NC, et al. Longitudinal lower airway microbial signatures of acute cellular rejection in lung transplantation. *Am J Respir Crit Care Med*. 2024;209:1463–1476. doi:10.1164/rccm.202309-1551OC.
17. McGinniss JE, Whiteside SA, Deek RA, et al. The lung allograft microbiome associates with pepsin, inflammation, and primary graft dysfunction. *Am J Respir Crit Care Med*. 2022;206:1508–1521. doi:10.1164/rccm.202112-2786OC.
18. Yu Y, Kim YH, Cho WH, et al. Unique changes in the lung microbiome following the development of chronic lung allograft dysfunction. *Microorganisms*. 2024;12:287. doi:10.3390/microorganisms12020287.
19. Watzenboeck ML, Gorki AD, Quattrone F, et al. Multi-omics profiling predicts allograft function after lung transplantation. *Eur Respir J*. 2022;59:2003292. doi:10.1183/13993003.03292-2020.
20. Sharma NS, Wille KM, Athira S, et al. Distal airway microbiome is associated with immunoregulatory myeloid cell responses in lung transplant recipients. *J Heart Lung Transplant*. 2017:S1053–2498(17)31898–31893. doi:10.1016/j.healun.2017.07.007.
21. Martin C, Mahan KS, Wiggen TD, et al. Microbiome and metabolome patterns after lung transplantation reflect underlying disease and chronic lung allograft dysfunction. *Microbiome*. 2024;12:196. doi:10.1186/s40168-024-01893-y.
22. Widder S, Görzer I, Friedel B, et al. Metagenomic sequencing reveals time, host, and body compartment-specific viral dynamics after lung transplantation. *Microbiome*. 2022;10:66. doi:10.1186/s40168-022-01244-9.
23. Abbas AA, Diamond JM, Chehoud C, et al. The perioperative lung transplant virome: torque teno viruses are elevated in donor lungs and show divergent dynamics in primary graft dysfunction. *J Heart Lung Transplant*. 2017;17:1313–1324. doi:10.1111/ajt.14076.
24. Lian Q, Song X, Yang J, et al. Alterations of lung microbiota in lung transplant recipients with pneumocystis jirovecii pneumonia. *Respir Res*. 2024;25:125. doi:10.1186/s12931-024-02755-9.
25. Påhlman LI, Manoharan L, Aspelund AS. Divergent airway microbiomes in lung transplant recipients with or without pulmonary infection. *Respir Res*. 2021;22:118. doi:10.1186/s12931-021-01724-w.
26. Gao R, Wang W, Qian T, et al. Pulmonary bacterial infection after lung transplantation: risk factors and impact on short-term mortality. *J Infect*. 2024;89:106273. doi:10.1016/j.jinf.2024.106273.
27. Ribeiro R, Samman A, Wang A, et al. Incidence of post-transplant cytomegalovirus viremia in patients receiving lungs after ex vivo lung perfusion. *JTCVS Open*. 2023;14:590–601. doi:10.1016/j.xjon.2023.02.008.
28. Neofytos D, Fishman JA, Horn D, et al. Epidemiology and outcome of invasive fungal infections in solid organ transplant recipients. *Transpl Infect Dis*. 2010;12:220–229. doi:10.1111/j.1399-3062.2010.00492.x.
29. Dettori M, Riccardi N, Canetti D, et al. Infections in lung transplanted patients: A review. *Pulmonology*. 2024;30:287–304. doi:10.1016/j.pulmoe.2022.04.010.
30. Belperio J, Palmer SM, Weigt SS. Host-pathogen interactions and chronic lung allograft dysfunction. *Ann Am Thorac Soc*. 2017;14:S242–S246. doi:10.1513/AnnalsATS.201606-464MG.
31. Fisher CE, Preiksaitis CM, Lease ED, et al. Symptomatic respiratory virus infection and chronic lung allograft dysfunction. *Clin Infect Dis*. 2016;62:313–319. doi:10.1093/cid/civ871.
32. Zou X, Yan M, Wang Y, et al. Accurate diagnosis of lower respiratory infections using host response and respiratory microbiome from a single metatranscriptome test of bronchoalveolar lavage fluid. *Adv Sci (Weinh)*. 2025;12:e2405087. doi:10.1002/advs.202405087.
33. Levine DJ, Glanville AR, Aboyoun C, et al. Antibody-mediated rejection of the lung: A consensus report of the International Society for Heart and Lung Transplantation. *J Heart Lung Transplant*. 2016;35:397–406. doi:10.1016/j.healun.2016.01.1223.
34. Husain S, Mooney ML, Danziger-Isakov L, et al. A 2010 working formulation for the standardization of definitions of infections in cardiothoracic transplant recipients. *J Heart Lung Transplant*. 2011;30:361–374. doi:10.1016/j.healun.2011.01.701.
35. Chen S, Zhou Y, Chen Y, Gu J. fastp: An ultra-fast all-in-one FASTQ preprocessor. *Bioinformatics*. 2018;34:i884–i890. doi:10.1093/bioinformatics/bty560.
36. McIver LJ, Abu-Ali G, Franzosa EA, et al. bioBakery: A meta'omic analysis environment. *Bioinformatics*. 2018;34:1235–1237. doi:10.1093/bioinformatics/btx754.
37. Wood DE, Lu J, Langmead B. Improved metagenomic analysis with Kraken 2. *Genome Biol*. 2019;20:257. doi:10.1186/s13059-019-1891-0.
38. Lu J, Breitwieser FP, Thielen P, Salzberg SL. Bracken: Estimating species abundance in metagenomics data. *Peer J Comput Sci*. 2017;3:e104. doi:10.7717/peerj-cs.104.
39. Li D, Liu CM, Luo R, Sadakane K, Lam TW. MEGAHIT: An ultra-fast single-node solution for large and complex metagenomics assembly via succinct de Bruijn graph. *Bioinformatics*. 2015;31:1674–1676. doi:10.1093/bioinformatics/btv033.
40. Li H, Durbin R. Fast and accurate short read alignment with Burrows-Wheeler transform. *Bioinformatics*. 2009;25:1754–1760. doi:10.1093/bioinformatics/btp324.
41. Danecek P, Bonfield JK, Liddle J, et al. Twelve years of SAMtools and BCFtools. *Gigascience*. 2021;10:giab008. doi:10.1093/gigascience/giab008.
42. Wang C, Zhang L, Jiang X, et al. Toward efficient and high-fidelity metagenomic data from sub-nanogram DNA: Evaluation of library preparation and decontamination methods. *BMC Biol*. 2022;20:225. doi:10.1186/s12915-022-01418-9.
43. Kassambara A, Mundt F. Factoextra: Extract and visualize the results of multivariate data analyses. R package. 2020. doi:10.32614/cran.package.factoextra.
44. Guénard G, Legendre P. Hierarchical clustering with contiguity constraint in R. J Statist Softw. 2022;103:1–26. doi:10.18637/jss.v103.i07.
45. Drost HG. Philentropy: Information theory and distance quantification with R. J Open Source Softw. 2018;3:765. doi:10.21105/joss.00765.
46. R Core Team. R: a language and environment for statistical computing. R Foundation for Statistical Computing, Vienna, Austria. Available from: https://www.R-project.org/. [Accessed on June 13, 2025].
47. Oksanen J, Kindt R, Lengendre P, et al. The vegan package. *Comm Ecol Package*. 2010;10:719. doi:10.32614/cran.package.vegan.
48. Yang L, Chen J. A comprehensive evaluation of microbial differential abundance analysis methods: Current status and potential solutions. *Microbiome*. 2022;10:130. doi:10.1186/s40168-022-01320-0.
49. Peschel S, Müller CL, von Mutius E, Boulesteix AL, Depner M. NetCoMi: Network construction and comparison for microbiome data in R. *Brief Bioinform*. 2021;22:bbaa290. doi:10.1093/bib/bbaa290.
50. Sinkkonen A, Roslund M, Skevaki C, Mmbaga BT, Nadeau KC, Renz H. Can we improve immune health by restoring microbial biodiversity? *Nat Rev Immunol*. 2025;25:477–478. doi:10.1038/s41577-025-01190-1.

51. Abdel-Aziz MI, Thorsen J, Hashimoto S, et al. Oropharyngeal microbiota clusters in children with asthma or wheeze associate with allergy, blood transcriptomic immune pathways, and exacerbation risk. *Am J Respir Crit Care Med*. 2023;208:142–154. doi:10.1164/rccm.202211-2107OC.
52. Zou X, Cao H, Hong L, et al. Enrichment of *Streptococcus* oralis in respiratory microbiome enhance innate immunity and protects against influenza infection. *Signal Transduct Target Ther*. 2025;10:272. doi:10.1038/s41392-025-02365-x.
53. Wohlfarth P, Leiner M, Schoergenhofer C, et al. Torquetenovirus dynamics and immune marker properties in patients following allogeneic hematopoietic stem cell transplantation: A prospective longitudinal study. *Biol Blood Marrow Transplant*. 2018;24:194–199. doi:10.1016/j.bbmt.2017.09.020.
54. Pradère P, Zajacova A, Bos S, Le Pavec J, Fisher A. Molecular monitoring of lung allograft health: Is it ready for routine clinical use. *Eur Respir Rev*. 2023;32:230125. doi:10.1183/16000617.0125-2023.
55. Paraskeva MA, Snell GI. Advances in lung transplantation: 60 years on. *Respirology*. 2024;29:458–470. doi:10.1111/resp.14721.
56. Jaksch P, Kundi M, Görzer I, et al. Torque teno virus as a novel biomarker targeting the efficacy of immunosuppression after lung transplantation. *J Infect Dis*. 2018;218:1922–1928. doi:10.1093/infdis/jiy452.
57. Kitsios GD, Yang H, Yang L, et al. Respiratory tract dysbiosis is associated with worse outcomes in mechanically ventilated patients. *Am J Respir Crit Care Med*. 2020;202:1666–1677. doi:10.1164/rccm.201912-2441OC.
58. Tony-Odigie A, Dalpke AH, Boutin S, Yi B. Airway commensal bacteria in cystic fibrosis inhibit the growth of *P. aeruginosa* via a released metabolite. *Microbiol Res*. 2024;283:127680. doi:10.1016/j.micres.2024.127680.
59. Sen Chaudhuri A, Sun J. Lung-resident lymphocytes and their roles in respiratory infections and chronic respiratory diseases. *Chin M J Pulm Crit Care Med*. 2024;2:214–223. doi:10.1016/j.pccm.2024.11.006.